Article

Mathematical Modeling of the Solid–Liquid Interface Propagation by the Boundary Integral Method with Nonlinear Liquidus Equation and Atomic Kinetics

Ekaterina A. Titova [1],*, **Dmitri V. Alexandrov** [2] and **Liubov V. Toropova** [1,3]

[1] Laboratory of Mathematical Modeling of Physical and Chemical Processes in Multiphase Media, Department of Theoretical and Mathematical Physics, Ural Federal University, Lenin Ave., 51, 620000 Ekaterinburg, Russia

[2] Laboratory of Multi-Scale Mathematical Modeling, Department of Theoretical and Mathematical Physics, Ural Federal University, Lenin Ave., 51, 620000 Ekaterinburg, Russia

[3] Otto-Schott-Institut für Materialforschung, Friedrich-Schiller-Universität-Jena, 07743 Jena, Germany

* Correspondence: eatitova@urfu.ru

Abstract: In this paper, we derive the boundary integral equation (BIE), a single integrodifferential equation governing the evolutionary behavior of the interface function, paying special attention to the nonlinear liquidus equation and atomic kinetics. As a result, the BIE is found for a thermodiffusion problem of binary melt crystallization with convection. Analyzing this equation coupled with the selection criterion for a stationary dendritic growth in the form of a parabolic cylinder, we show that nonlinear effects stemming from the liquidus equation and atomic kinetics play a decisive role. Namely, the dendrite tip velocity and diameter, respectively, become greater and lower with the increasing deviation of the liquidus equation from a linear form. In addition, the dendrite tip velocity can substantially change with variations in the power exponent of the atomic kinetics. In general, the theory under consideration describes the evolution of a curvilinear crystallization front, as well as the growth of solid phase perturbations and patterns in undercooled binary melts at local equilibrium conditions (for low and moderate Péclet numbers). In addition, our theory, combined with the unsteady selection criterion, determines the non-stationary growth rate of dendritic crystals and the diameter of their vertices.

Keywords: boundary integral equation; phase transitions; curved solid–liquid interface; undercooled melt

1. Introduction

The dynamics of curved phase transition fronts moving in undercooled binary mixtures completely characterizes the birth of material structures that appear as a result of the phase transformation process. This dynamic behavior of such fronts under the influence of external forces also defines the evolution of morphological perturbations, the appearance and growth of interfacial ridges, and the formation of a two phase layer that divides the material phases [1–6]. An important point is that the curved phase interface is usually considered to be mesoscopically or macroscopically acute.

Let us introduce the interface function $z_{\text{interface}} = \zeta(\mathbf{x}, t)$ characterizing the position and velocity of a curvilinear phase transition front (see also Figure 1). This function satisfies the boundary-integral equation deduced in [7,8] for purely thermal problem and then extended in [9,10] for some solid–solid and fluid–fluid systems. Here, $\mathbf{x} = (x, y)$ and t stand for the vector of spatial coordinates and the time variable. Note that this method enables obtaining the boundary-integral equation for the interface function when considering the phase interface propagation in purely thermal or concentration problems in the absence of convection. Considering the thermal and concentration fields synchronously (an undercooled binary mixture), the authors of [11–13] extended the aforementioned approach for

slow, moderate, and fast crystallization phenomena. On the other hand, the purely thermal theory [7,8] has been extended to the case of interface propagation in one-component and binary undercooled melts in the presence of a forced convective flow [14,15]. In this paper, the boundary integral theory is developed for the case of the nonlinear liquidus equation containing the kinetic contribution, which plays an important role with the increasing phase interface velocity. Strictly speaking, a new boundary-integral equation (BIE) for the interface function that describes the propagation of a curvilinear front into a binary undercooled mixture is derived. This BIE also describes the evolution of morphological perturbations of the solid–liquid phase interface arising as a result of temperature fluctuations or some external reasons [16]. What is more, the BIE under question characterizes how solid phase ridges or patterns can evolve into an undercooled melt and form complex material structures.
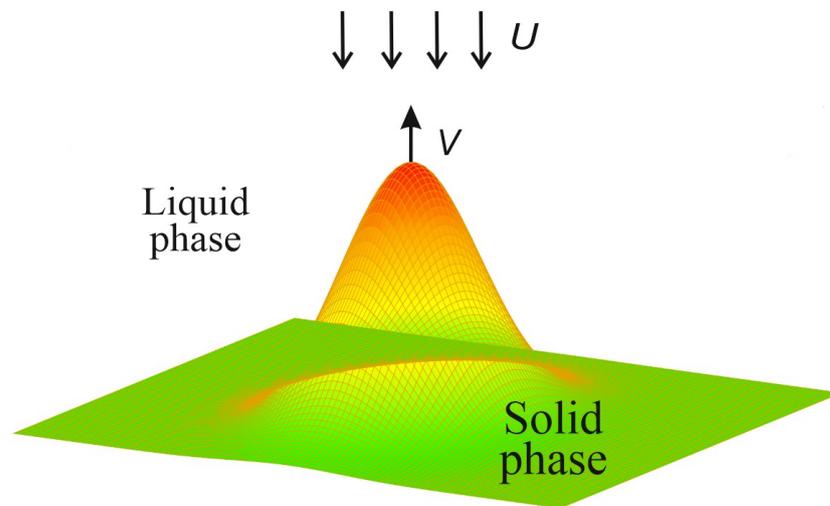
Figure 1. A sketch of the curvilinear solid–liquid interface.

2. The Model and BIE for the Interface Function

2.1. The Heat and Mass Transfer Model

The heat transfer equation for the liquid–solid (bulk) phases and the solute diffusion equation in the liquid phase can be written as

$$\frac{\partial T_d}{\partial t} + (\mathbf{u} \cdot \nabla)T_d - V\frac{\partial T_d}{\partial z} = D_T \nabla^2 T_d, \tag{1}$$

$$\frac{\partial C_d}{\partial t} + (\mathbf{u} \cdot \nabla)C_d - V\frac{\partial C_d}{\partial z} = D_C \nabla^2 C_d, \tag{2}$$

where T_d is the melt temperature, C_d is the solute concentration, $\mathbf{u}$ is the melt velocity, D_T is the thermal conductivity, D_C is the diffusion coefficient, and V is a constant velocity of the Cartesian coordinate system x, y, and z (steady-state growth rate).

The temperature, solute concentration, and fluid velocity are fixed far from the phase transition interface, $T_d = T_{d\infty}$, $C_d = C_{d\infty}$, $\mathbf{u} = -U_\infty$, and the boundary conditions at the solid–liquid interface take the form of

$$T_d = T_{d0} - d_c \mathcal{K}_d \frac{Q}{c_p} + m_1 C_d + m_2 C_d^2 - \beta_k \left(V + \frac{\partial \zeta}{\partial t}\right)^n, \quad \mathbf{u} = 0,$$

$$D_T \left(\nabla T_{d\ solid} - \nabla T_{d\ liquid}\right) \cdot d\mathbf{s} = \frac{Q}{c_p}\left(V + \frac{\partial \zeta}{\partial t}\right)d^2 x,$$

$$-D_C \nabla C_d \cdot d\mathbf{s} = (1 - k_0)C_d\left(V + \frac{\partial \zeta}{\partial t}\right)d^2 x, \tag{3}$$

where $d_c = d_0[1 - \alpha_d \cos(\iota\theta)]$ is the anisotropy capillary length, d_0 is the capillary constant, $\alpha_d \ll 1$ is the stiffness parameter, θ is the angle expressing the orientation between the normal and growth direction, ι is the order of the crystalline symmetry, $\mathcal{K}_d$ is the average curvature of the interface, Q is the latent heat of crystallization, m_1 is the liquidus line slope, m_2 is the deviation of the liquidus equation from a linear form [17], c_p is the heat capacity, β_k is the kinetic coefficient, n is the power exponent of the atomic kinetics, T_{d0} is the phase transition temperature for the flat front, $d\mathbf{s}$ is the surface area vector element directed toward the liquid phase, k_0 is the solute partition coefficient, and ζ is the interface function. The average curvature of the interface $\mathcal{K}_d$ in the two-dimensional case can be determined as

$$\mathcal{K}_d(x,t) = -\frac{\partial^2 \zeta(x,t)/\partial x^2}{\left(1 + (\partial \zeta(x,t)/\partial x)^2\right)^{3/2}}. \tag{4}$$

In this section, we derive an integrodifferential equation for the interface function $\zeta(x,t)$ in the case of the thermo-diffusion problem with convection (1)–(4). For convenience, let us introduce the characteristic length $2D_T/V$ and time $4D_T/V^2$ scales, as well as dimensionless temperature $T = T_d c_p/Q$, solute concentration $C = m_1 c_p C_d/Q$, and fluid velocity $\mathbf{v} = \mathbf{u}/U_\infty$.

Thus, the dimensionless model of convective heat and mass transfer following from (1) and (2) has the form:

$$\frac{\partial T}{\partial t} + 2\frac{U_\infty}{V}(\mathbf{v} \cdot \nabla)T - 2\frac{\partial T}{\partial z} - \nabla^2 T = 0, \tag{5}$$

$$\frac{\partial C}{\partial t} + 2\frac{U_\infty}{V}(\mathbf{v} \cdot \nabla)C - 2\frac{\partial C}{\partial z} - \frac{D_C}{D_T}\nabla^2 C = 0, \tag{6}$$

where $\mathbf{v}$ is the dimensionless velocity. The boundary conditions read as

$$T = T_i = T_0 - \frac{d_c KV}{2D_T} + C_i + \frac{Qm_2}{m_1^2 c_p}C_i^2 - \beta\left(2 + \frac{\partial\zeta}{\partial t}\right)^n \quad \text{at } \zeta, \tag{7}$$

$$\left(\nabla T_{solid} - \nabla T_{liquid}\right) \cdot d\mathbf{s} = \left(2 + \frac{\partial\zeta}{\partial t}\right)d^2 x \quad \text{at } \zeta, \tag{8}$$

$$-\frac{D_C}{D_T}\nabla C_{liquid} \cdot d\mathbf{s} = (1 - k_0)C_i\left(2 + \frac{\partial\zeta}{\partial t}\right)d^2 x \quad \text{at } \zeta, \tag{9}$$

$$T = T_\infty, \quad C = C_\infty, \quad \mathbf{v} = 1 \quad \text{at infinity}, \tag{10}$$

where $\beta = \beta_k c_p V^n/(2^n Q)$ and subscript i corresponds to the interface.

2.2. The Green's Function Technique

Let us use Green's functions $G_T(\mathbf{p}|\mathbf{p}_1)$ and $G_C(\mathbf{p}|\mathbf{p}_1)$ for the heat transfer and diffusion equations without flow to solve the convective problem (5)–(10):

$$\frac{\partial G_T}{\partial t_1} + \nabla_1^2 G_T - 2\frac{\partial G_T}{\partial z_1} = -\delta(\mathbf{p} - \mathbf{p}_1), \quad \frac{\partial G_C}{\partial t_1} + \frac{D_C}{D_T}\nabla_1^2 G_C - 2\frac{\partial G_C}{\partial z_1} = -\delta(\mathbf{p} - \mathbf{p}_1), \tag{11}$$

where $\mathbf{p} = (x,z,t)$ and $\mathbf{p}_1 = (x_1, z_1, t_1)$.

Green's functions for heat $G_T(\mathbf{p}|\mathbf{p}_1)$ and chemical $G_C(\mathbf{p}|\mathbf{p}_1)$ problems can be obtained using the Fourier transform (see, among others, [9–11,18]) and read as

$$G_T(\mathbf{p}|\mathbf{p}_1) = \frac{1}{[4\pi(t-t_1)]^{3/2}} \exp\left(-\frac{|x-x_1|^2 + [z-z_1+2(t-t_1)]^2}{4(t-t_1)}\right), \tag{12}$$

$$G_C(\mathbf{p}|\mathbf{p}_1) = \left(\frac{D_T}{4\pi(t-t_1)D_C}\right)^{3/2} \exp\left(-D_T \frac{|x-x_1|^2 + (z-z_1+2(t-t_1))^2}{4(t-t_1)D_C}\right). \tag{13}$$

By multiplying Equations (5) and (6) at $\mathbf{p}_1$ by $G_T(\mathbf{p}|\mathbf{p}_1)$ and $G_C(\mathbf{p}, \mathbf{p}_1)$ and Equation (11) by $T(\mathbf{p}_1)$ and $C(\mathbf{p}_1)$, respectively, subtracting one from the other and integrating the result over $\mathbf{p}_1$, we obtain the temperature and solute concentration in liquid:

$$T(\mathbf{p}) = \int_{-\infty}^{t+\varepsilon}\int_{\Lambda_1} dt_1 dx_1 dz_1 \left(2\frac{\partial(G_T T)}{\partial z_1} - 2G_T \frac{U_\infty}{V}(\mathbf{v}\cdot\nabla_1)T - \frac{\partial(G_T T)}{\partial t_1}\right)$$

$$+ \int_{-\infty}^{t+\varepsilon}\int_{\Lambda_1} dt_1 dx_1 dz_1 \left(G_T \nabla_1^2 T - T\nabla_1^2 G_T\right), \tag{14}$$

$$C(\mathbf{p}) = \int_{-\infty}^{t+\varepsilon}\int_{\Lambda_1} dt_1 dx_1 dz_1 \left(2\frac{\partial(G_C C)}{\partial z_1} - 2G_C \frac{U_\infty}{V}(\mathbf{v}\cdot\nabla_1)C - \frac{\partial(G_C C)}{\partial t_1}\right)$$

$$+ \frac{D_C}{D_T}\int_{-\infty}^{t+\varepsilon}\int_{\Lambda_1} dt_1 dx_1 dz_1 \left(G_C \nabla_1^2 C - C\nabla_1^2 G_C\right), \tag{15}$$

where Λ_1 contains the point (x,z) and ε represents a small positive parameter.

The integrals of the time derivatives in Equations (14) and (15) turn to zero after integration over time t_1. In this case, Green's functions also tend to zero, and the temperature and concentration are bounded at the lower limit of integration. Moreover, the Green function is equal to zero at the upper limit because of the causality condition [18]. In addition, the integrals of the z_1-derivative over z_1 in Equations (14) and (15) give a constant temperature T_∞ and concentration C_∞. Next, applying Green's theorem, substituting the heat and mass boundary conditions (8) and (9) into (14) and (15), extending the point $\mathbf{p}$ to the phase transition surface, and taking $\varepsilon \to 0$, we arrive at

$$\int_{-\infty}^{t}\int_{-\infty}^{\infty} dt_1 dx_1 \left(G_T(\mathbf{p}^\zeta|\mathbf{p}_1^\zeta)\left(2 + \frac{\partial\zeta}{\partial t}\right)\right)$$

$$-2\frac{U_\infty}{V}\int_{-\infty}^{t}\int_{\Lambda_1} dt_1 dx_1 dz_1 G_T(\mathbf{v}\cdot\nabla_1)T = T_i - T_\infty, \tag{16}$$

$$(1-k_0)\int_{-\infty}^{t}\int_{-\infty}^{\infty} dt_1 dx_1 \left(C_i G_C(\mathbf{p}^\zeta|\mathbf{p}_1^\zeta)\left(2 + \frac{\partial\zeta}{\partial t}\right)\right)$$

$$-2\frac{U_\infty}{V}\int_{-\infty}^{t}\int_{\Lambda_1} dt_1 dx_1 dz_1 G_C(\mathbf{v}\cdot\nabla_1)C = C_i - C_\infty. \tag{17}$$

Here, the superscript ζ defines the phase interface. Let us write down the Gibbs–Thomson condition for the isothermal growth with the concentration gradient in the form of

$$\frac{d_c KV}{2D_T} + \beta\left(2 + \frac{\partial\zeta}{\partial t}\right)^n = C_i + \frac{Qm_2}{m_1^2 c_p}C_i^2. \tag{18}$$

The solution to this equation relative to C_i yields two real roots. One of them determining the interfacial concentration is positive and is given by

$$C_i = m_1^2 c_p \frac{\sqrt{1 + 4\frac{Qm_2}{m_1^2 c_p}\left[\beta\left(2 + \frac{\partial\zeta}{\partial t}\right)^n + \frac{d_c KV}{2D_T}\right]} - 1}{2Qm_2}. \tag{19}$$

Thus, Equations (17) and (19) together determine the growth of an isothermal dendrite from solution. For the combined thermal and concentration problem, let us now substitute T_i and C_i expressed in Equations (16) and (17) into the Gibbs–Thomson Equation (7). The result reads as

$$2\int\limits_{-\infty}^{t}\int\limits_{-\infty}^{\infty} dt_1 dx_1 \left(G_T(\mathbf{p}^\zeta|\mathbf{p}_1^\zeta)\left(2 + \frac{\partial\zeta}{\partial t}\right)\right) - 2\frac{U_\infty}{V}\int\limits_{-\infty}^{t}\int\limits_{\Lambda_1} dt_1 dx_1 dz_1 G_T(\mathbf{v}\cdot\nabla_1)T$$

$$= \Delta - \frac{d_c KV}{2D_T} + C_i + \frac{Qm_2}{m_1^2 c_p}C_i^2 - \beta\left(2 + \frac{\partial\zeta}{\partial t}\right)^n, \tag{20}$$

where C_i is defined by Equation (17). Thus, Equation (20) represents an integrodifferential equation for the interface function $\zeta(\mathbf{x}, t)$ satisfying the convective problem (5)–(10) and describing the phase interface dynamics for purely thermal and thermo-concentration problems with convection with allowance for nonlinear liquidus equation and atomic kinetics. Let us especially note that the second term on the left-hand side of Equation (20) takes the flow into account.

2.3. Stationary Growth

In the case of stationary growth, the BIE transforms to

$$\int\limits_{-\infty}^{t}\int\limits_{-\infty}^{\infty} G_T(\mathbf{p}^\zeta|\mathbf{p}_1^\zeta)dt_1 dx_1 - 2\frac{U_\infty}{V}\int\limits_{-\infty}^{t}\int\limits_{\Lambda_1} dt_1 dx_1 dz_1 G_T(\mathbf{v}\cdot\nabla_1)T$$

$$= \Delta - \frac{d_c KV}{2D_T} + C_i + \frac{m_2}{m_1}C_i^2 - 2^n\beta,$$

$$C_i = \frac{C_\infty - 2\frac{U_\infty}{V}\int\limits_{-\infty}^{t}\int\limits_{\Lambda_1} dt_1 dx_1 dz_1 G_C(\mathbf{v}\cdot\nabla_1)C}{1 - 2(1-k_0)\int\limits_{-\infty}^{t}\int\limits_{-\infty}^{\infty} dt_1 dx_1 \left(G_C(\mathbf{p}^\zeta|\mathbf{p}_1^\zeta)\right)}. \tag{21}$$

Here, $\Delta = T_0 - T_\infty$ is the dimensionless undercooling and the solute concentration in solid is constant. In the case of stationary growth, the only time-dependent function is Green's function, and we can integrate it over time for the thermal problem:

$$\int\limits_{-\infty}^{t} G_T(\mathbf{p}^\zeta|\mathbf{p}_1^\zeta)dt_1 = \frac{1}{2\pi}\exp(z_1 - z)K_0\left(\frac{\sqrt{(x - x_1)^2 + (z - z_1)^2}}{2}\right), \tag{22}$$

where K_0 is the modified Bessel function. For the concentration problem, the integral over time can be written as

$$\int_{-\infty}^{t} G_C(\mathbf{p}^{\zeta}|\mathbf{p}_1^{\zeta}) dt_1 = \exp\left(\frac{z_1 - z}{D_C/D_T}\right) \frac{D_T}{2\pi D_C} K_0\left(\frac{\sqrt{(x - x_1)^2 + (z - z_1)^2}}{2D_C/D_T}\right). \tag{23}$$

Now, we obtain a general solution for the growth of any stationary form by substituting the thermal and concentration integrals of Green's function:

$$\frac{1}{\pi} \int_{-\infty}^{\infty} \exp(\zeta - \zeta_1) K_0\left(\frac{\sqrt{(x - x_1)^2 + (\zeta - \zeta_1)^2}}{2}\right) dx_1$$

$$-\lambda \frac{1}{\pi} \int_{-\infty}^{\infty} \int_{\zeta}^{\infty} \exp(z_1 - z) K_0\left(\frac{\sqrt{(x - x_1)^2 + (z_1 - z)^2}}{2}\right) \mathbf{v} \cdot \nabla T dx_1 dz_1$$

$$= T_0 - T_\infty - \frac{d_c K V}{2D_T} + C_i + \frac{m_2 Q}{m_1 c_p} C_i^2 - 2\beta, \tag{24}$$

where

$$C_i = \frac{\frac{\lambda}{\pi} \frac{D_T}{D_C} \int_{-\infty}^{\infty} \int_{\zeta}^{\infty} \exp\left(\frac{z_1 - z}{D_C/D_T}\right) K_0\left(\frac{\sqrt{(x - x_1)^2 + (z - z_1)^2}}{2D_C/D_T}\right) \mathbf{v} \cdot \nabla C dx_1 dz_1 - C_\infty}{\frac{1 - k_0}{\pi} \frac{D_T}{D_C} \int_{-\infty}^{\infty} \exp\left(\frac{\zeta_1 - \zeta}{D_C/D_T}\right) K_0\left(\frac{\sqrt{(x - x_1)^2 + (\zeta - \zeta_1)^2}}{2D_C/D_T}\right) dx_1 - 1}.$$

2.4. The Parabolic Cylinder Reference Frame

Let us introduce the two-dimensional parabolic coordinates [14,19]:

$$w = \left(\sqrt{x^2 + z^2} + z\right)/p_T, \quad s = \left(\sqrt{x^2 + z^2} - z\right)/p_T, \tag{25}$$

where $p_T = \rho V/(2D_T)$ is the Péclet number and ρ is the crystal tip diameter.

The integrals of Green's function were previously calculated in [12] as

$$2\int_{-\infty}^{t} \int_{-\infty}^{\infty} dt_1 dx_1 \left(G_T(\mathbf{p}^{\zeta}|\mathbf{p}_1^{\zeta})\right) = \sqrt{p_T \pi} \exp(p_T) \text{erfc}(\sqrt{p_T})$$

and

$$2\int_{-\infty}^{t} \int_{-\infty}^{\infty} dt_1 dx_1 \left(G_C(\mathbf{p}^{\zeta}|\mathbf{p}_1^{\zeta})\right) = \sqrt{p_C \pi} \exp(p_C) \text{erfc}(\sqrt{p_C}).$$

Next, we use the Jacobian J and replace the variables z_1 and x_1 in the convective integral of Equation (21) with the variables w_1 and s_1 defined by Equation (25):

$$J = \begin{vmatrix} \dfrac{\partial x}{\partial w} & \dfrac{\partial x}{\partial s} \\ \dfrac{\partial z}{\partial w} & \dfrac{\partial z}{\partial s} \end{vmatrix} = -\frac{p_T^2}{4}\left(\frac{\sqrt{s}}{\sqrt{w}} + \frac{\sqrt{w}}{\sqrt{s}}\right). \tag{26}$$

Therefore, replacing the variables in (21), we obtain

$$
\int_{-\infty}^{t}\int_{-\infty}^{\infty}\int_{\zeta_1}^{\infty} dt_1 dx_1 dz_1 G_T(\mathbf{p}^\zeta|\mathbf{p}_1)(\mathbf{v}\cdot\nabla_1)T
$$

$$
=\int_{-\infty}^{t}\int_{-\infty}^{\infty}\int_{1}^{\infty} dt_1 ds_1 dw_1 J G_T(\mathbf{p}^\zeta|\mathbf{p}_1)(\mathbf{v}\cdot\nabla_1)T. \tag{27}
$$

Note that the convective integral contribution stemming from the solute concentration has the same form. The next step in our calculations is to obtain the temperature gradient. To do this, let us rewrite the heat conduction equation in parabolic coordinates as

$$
\frac{d^2 T}{dw^2} = \frac{dT}{dw}\left(p_T \frac{U_\infty}{V} v_w \sqrt{\frac{w+s}{w}} - p_T - \frac{1}{2w}\right). \tag{28}
$$

Integrating Equation (28) and taking the heat balance boundary condition into account, we express the convective term as

$$
(\mathbf{v}\cdot\nabla)T = v_w \frac{2}{p_T}\sqrt{\frac{w}{w+s}}\frac{dT}{dw}
$$

$$
= -2v_w\sqrt{\frac{1}{w(w+s)}}\exp\left(\int_{1}^{w}\left(p_T\frac{U_\infty}{V}v_w\sqrt{\frac{w+s}{w}} - p_T\right)dw_1\right). \tag{29}
$$

The hydrodynamic field was found in [20,21] and reads as

$$
v_w\sqrt{\frac{w+s}{w}} = v_2 = \frac{\operatorname{erfc}\left(\sqrt{Re\frac{w}{2}}\right) + \frac{2}{\pi Rew}\left(\exp\left(-\frac{Re}{2}\right) - \exp\left(-w\frac{Re}{2}\right)\right)}{\operatorname{erfc}\left(\sqrt{\frac{Re}{2}}\right)} - 1, \tag{30}
$$

where $Re = \rho U_\infty/\nu$ is the Reynolds number and ν is the kinematic viscosity.

Now, substituting (29) into (27), we obtain

$$
\int_{-\infty}^{t}\int_{-\infty}^{\infty}\int_{1}^{\infty} dt_1 ds_1 dw_1 J G_T(\mathbf{p}^\zeta|\mathbf{p}_1)(\mathbf{v}\cdot\nabla_1)T
$$

$$
= \frac{p_T^2}{2}\int_{-\infty}^{t}\int_{-\infty}^{\infty}\int_{1}^{\infty} dt_1 ds_1 dw_1 G_T(\mathbf{p}^\zeta|\mathbf{p}_1)\frac{v_2}{\sqrt{ws}}\exp\left(\int_{1}^{w}\left(p_T\frac{U_\infty}{V}v_2 - p_T\right)dw_1\right). \tag{31}
$$

The last step is to integrate the Green's function derived in [15]. The result reads as

$$
\int_{-\infty}^{t}\int_{-\infty}^{\infty} G_T(\mathbf{p}^\zeta|\mathbf{p}_1)dt_1\frac{ds_1}{\sqrt{s_1}} = \frac{\sqrt{p_T w_1 \pi}}{2}\exp(p_T w_1)\operatorname{erfc}(\sqrt{p_T w_1}) \tag{32}
$$

for the thermal and

$$
\int_{-\infty}^{t}\int_{-\infty}^{\infty} G_C(\mathbf{p}^\zeta|\mathbf{p}_1)dt_1\frac{ds_1}{\sqrt{s_1}} = \frac{\sqrt{p_C w_1 \pi}}{2}\exp(p_C w_1)\operatorname{erfc}(\sqrt{p_C w_1}) \tag{33}
$$

for the concentration contributions. Finally, we obtain the convective boundary integral equation for a dendrite having the form of a parabolic cylinder and growing with a constant velocity in an undercooled binary melt:

$$\sqrt{p_T\pi}\exp(p_T)\left[\mathrm{erfc}(\sqrt{p_T})-\frac{p_T^2}{2}\int_1^\infty\sqrt{w_1}\mathrm{erfc}(\sqrt{p_Tw_1})v_2(w_1)\exp\left(p_T\int_1^{w_1}v_2(w_2)dw_2\right)dw_1\right.$$

$$=T_0-T_\infty-\frac{d_cKV}{2D_T}+C_i+\frac{m_2Q}{m_1c_p}C_i^2-2\beta,\tag{34}$$

$$C_i=\frac{p_T^2\frac{\sqrt{\pi p_C}}{2}\exp(p_C)\int_1^\infty\sqrt{w_1}\mathrm{erfc}(\sqrt{p_Cw_1})v_2(w_1)\exp\left(p_C\int_1^{w_1}v_2(w_2)dw_2\right)dw_1-C_\infty}{2(1-k_0)\sqrt{\pi p_C}\exp(p_C)\mathrm{erfc}(\sqrt{p_C})-1}\left.\vphantom{\int}\right]$$

As a special note, Equation (34) contains the fluid flow in terms of v_2, which is dependent on the Reynolds number $Re(U_\infty)$ (see Equation (30)).

3. Numerical Examples

The selection criterion $\sigma^*=2d_0D_T/(\rho^2V)$ for the 2D thermo-solutal dendritic growth with convection and surface tension anisotropy is defined by [21]

$$\sigma^*=\frac{\sigma_0\alpha_d^{7/4}}{1+b\left(\alpha\alpha_d^{-3/4}\right)^{11/14}}\left[\frac{1}{\left(1+a_1\sqrt{\alpha_d}p_T\right)^2}-\frac{1}{\left(1+a_2\sqrt{\alpha_d}p_TD_T/D_C\right)^2}\frac{2m_1C_i(1-k_0)D_T}{(Q/c_p)D_C}\right],\tag{35}$$

$$\alpha=\left(\frac{ad_0U_\infty}{4\rho V}+\frac{ad_0U_\infty D_T}{2\rho VD_C}\right)\left(1-\frac{2m_1C_i(1-k_0)D_T}{D_CQ/c_p}\right),\quad a(\mathrm{Re})=\sqrt{\frac{\mathrm{Re}}{2\pi}}\frac{\exp(-\mathrm{Re}/2)}{\mathrm{erfc}\left(\sqrt{\mathrm{Re}/2}\right)},$$

where σ_0 is the selection constant, b is the selection parameter responsible for fluid flow, $a_1=(8\sigma_0/7)^{1/2}(3/56)^{3/8}$, $a_2=\sqrt{2}a_1$, $\alpha_d=15\varepsilon_c$, and ε_c is the surface energy anisotropy. The selection criterion (35) describes the stable growth mode of a dendritic crystal with a constant velocity in an undercooled binary melt with a forced flow. As this takes place, the first term in square brackets represents the thermal contribution; the second term is the contribution from the solute concentration; the term containing coefficient b is responsible for the incoming flow; the terms containing the Péclet numbers p_T describe crystallization with an increased velocity. In general, Formula (35) works for low and moderate Péclet numbers in local-equilibrium conditions. When dealing with the local-nonequilibrium scenario that occurs for high crystal growth velocities (Péclet numbers), the corresponding high-speed selection criterion should be used [13,22].

Figure 2 shows the influence of the nonlinear liquidus slope (coefficient m_2) on the crystal velocity—melt undercooling and tip diameter melt undercooling curves. As would be expected, the velocity V builds up, and the diameter ρ reduces with increasing the melt undercooling. As this takes place, V and ρ, respectively, become greater and lower with increasing the deviation m_2 of the liquidus equation from a linear form. Therefore, for example, choosing the melt undercooling $\Delta=75$ K (right panel in Figure 2), we see that the dendrite tip diameter changes within the range of 20% when the tip radius varies between $\sim4\times10^{-6}$ m ($m_2=8$ K (at.%)$^{-2}$) and $\sim5\times10^{-6}$ m ($m_2=0$). This significantly changes the alloy microstructure (e.g., the primary interdendritic spacing [23–25]). The influence of the power exponent of the atomic kinetics n on $V(\Delta)$ and $\rho(\Delta)/2$ is illustrated in Figure 3. As is easily seen, the crystal growth velocity V can change up to 60% (compare the red and green curves at $\Delta=200$ K). This means a great impact of the atomic kinetic law on the crystallization rate.

In general, the BIE developed in this paper describes a broader class of undercooled crystallizing binary systems with a moving interphase boundary than previously known theories. This is explained by taking into account the nonlinear dependence of the phase transition temperature on the dissolved impurity concentration and the power law for the kinetics of particle attachment to the solidification front.
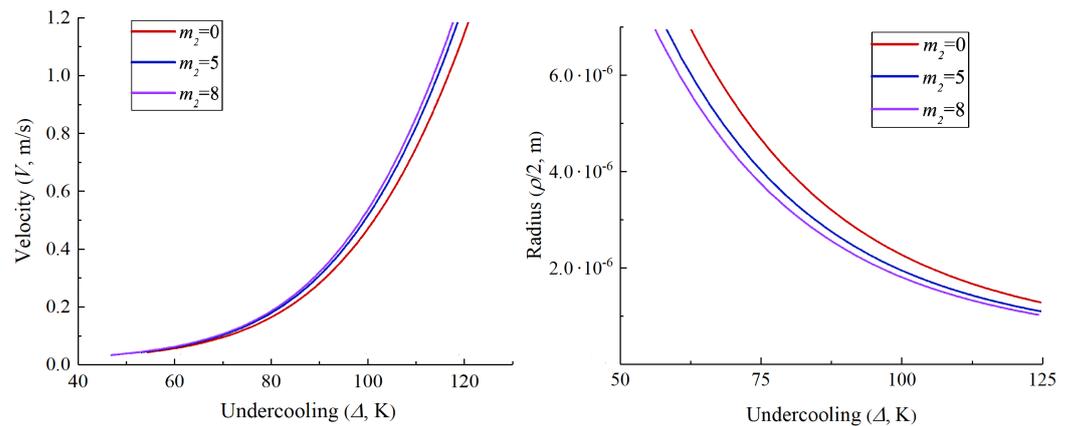
Figure 2. Dendrite tip velocity V and radius $\rho/2$ as functions of the melt undercooling Δ for the TiAl alloy. The colored lines represent the effect of quadratic liquidus m_2. The parameters used in the calculation are: solidification temperature $T_{d0} = 1748$ K, hypercooling $T_Q = 272$ K, impurity concentration $C_{d\infty} = 55$ at.%, distribution coefficient $k_0 = 0.8$, liquidus slope $m_1 = -8.8$ K (at.%)$^{-1}$, diffusion coefficient in liquid $D_C = 8.27 \times 10^{-9}$ m^2 s^{-1}, temperature diffusivity $D_T = 7.5 \times 10^{-6}$ m^2 s^{-1}, kinematic viscosity of the liquid $\nu = 0.5 \times 10^{-7}$ m^2 s^{-1}, fluid velocity $U_\infty = 0.1$ m s^{-1}, latent heat of solidification $Q = 12268.8$ J mol^{-1}, heat capacity $c_p = 45$ J (mol K)$^{-1}$, capillary length $d_c \approx d_0 = 7.8 \times 10^{-10}$ m, kinetic coefficient $\beta_k = 0.2$ m (s K)$^{-1}$, power exponent of the atomic kinetics $n = 1$, surface energy anisotropy $\varepsilon_c = 0.01$, selection constant $\sigma_0 = 0.05$, selection parameter responsible for fluid flow $b = 0.1$. The coefficient m_2 shown in the figure inserts is measured in K (at.%)$^{-2}$.
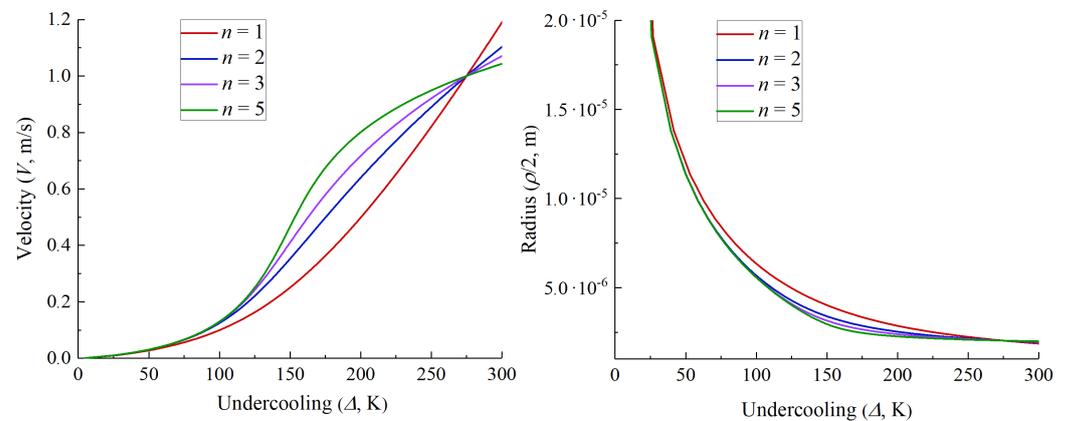
Figure 3. Dendrite tip velocity V and radius $\rho/2$ as functions of the melt undercooling Δ for the pure Ni alloy. The colored lines represent the effect of different powers of the atomic kinetics exponent n. The parameters used in the calculation: solidification temperature $T_{d0} = 1728$ K, hypercooling $T_Q = 435$ K, temperature diffusivity $D_T = 1 \times 10^{-5}$ m^2 s^{-1}, kinematic viscosity of the liquid $\nu = 7.14 \times 10^{-7}$ m^2 s^{-1}, fluid velocity $U_\infty = 0.001$ m s^{-1}, capillary length $d_c \approx d_0 = 4.2 \times 10^{-10}$ m, kinetic coefficient $\beta_k = 0.01$ m (s K)$^{-1}$, surface energy anisotropy $\varepsilon_c = 0.02$, selection constant $\sigma_0 = 0.05$, selection parameter responsible for fluid flow $b = 0.1$.

4. Conclusions

In summary, in this study, we developed the boundary integral theory with allowance for the nonlinear liquidus equation with a kinetic contribution playing a significant role with the increasing phase interface velocity. The boundary integral equation, a single integrodifferential equation for the interface function, was derived for the thermo-concentration problem, which describes a solidification process of an undercooled binary melt in the presence of convection. This equation characterizes the motion of the curved solid–liquid interface (solidification front) propagating into an undercooled liquid phase in cases of small and moderate crystallization velocities (Péclet numbers) [26]. Our calculations of the

boundary integral based on a parabolic tip shape of the dendritic crystal showed that a nonlinear contribution to the liquidus equation (the term proportional to the square of the solute concentration) and the power exponent of the atomic kinetics can essentially change the interface velocity—melt undercooling curve for moderate values of $\Delta T \sim 50$–250 K. With the further increase of the undercooling, the developed theory has to be generalized to the case of the hyperbolic impurity diffusion equation [27,28].

As a special note, the boundary integral equation under consideration has great potential applications for the further development of crystallization theory. For example, it can be used for simulating the pattern formation and crystal growth in undercooled liquids [12,29], studying the development of morphological instability [2,9,10,30], and deriving a selection criterion for a stable mode of dendritic growth [1,21,30]. An important task of crystallization theory is to derive the boundary integral while taking into account the nucleation and growth of particles in an undercooled liquid ahead of the phase transformation boundary. This problem can be solved by combining the present analysis and the theory of crystal growth at the intermediate stage of phase transformation [31–38]. Another important task is to determine the boundary integral equation for the directional crystallization process with a two-phase region. Such a problem can be attempted by combining the theory under consideration and the crystallization theory with a quasi-equilibrium two phase region [39–44]. The method of the boundary integral equation developed in this paper can also be applied to describe moving boundaries in biologically active media [45,46], as well as in complex heterogeneous systems of different physical natures [47,48].

Author Contributions: Conceptualization, E.A.T. and D.V.A.; methodology, E.A.T. and D.V.A.; software, L.V.T. and E.A.T.; validation, L.V.T. and E.A.T.; formal analysis, E.A.T. and D.V.A.; investigation, E.A.T.; resources, E.A.T. and L.V.T.; writing—original draft preparation, E.A.T., D.V.A. and L.V.T.; writing—review and editing, E.A.T., D.V.A. and L.V.T.; visualization, L.V.T.; supervision, D.V.A. All authors have read and agreed to the published version of the manuscript.

Data Availability Statement: All data generated or analyzed during this study are included in this published article.

Conflicts of Interest: The authors declare no conflict of interest.

References

1. Pelcé, P. *Dynamics of Curved Fronts*; Academic Press: Boston, MA, USA, 1988.
2. Kessler, D.A.; Koplik, J.; Levine, H. Pattern selection in fingered growth phenomena. *Adv. Phys.* **1988**, *37*, 255–339. [CrossRef]
3. Almgren, R.; Dai, W.-S.; Hakim, V. Scaling behavior in anisotropic Hele–Shaw flow. *Phys. Rev. Lett.* **1993**, *71*, 3461–3464. [CrossRef] [PubMed]
4. Alexandrov, D.V. Self-similar solidification: Morphological stability of the regime. *Int. J. Heat Mass Trans.* **2004**, *47*, 1383–1389. [CrossRef]
5. Alexandrov, D.V.; Ivanov, A.A. Solidification of a ternary melt from a cooled boundary, or nonlinear dynamics of mushy layers. *Int. J. Heat Mass Trans.* **2009**, *52*, 4807–4811. [CrossRef]
6. Alexandrov, D.V.; Nizovtseva, I.G.; Malygin, A.P.; Huang, H.-N.; Lee, D. Unidirectional solidification of binary melts from a cooled boundary: Analytical solutions of a nonlinear diffusion-limited problem. *J. Phys. Condens. Matter* **2008**, *20*, 114105. [CrossRef]
7. Nash, G.E. Capillary-limited, steady state dendritic growth. Part I. Theoretical development. *NRL Rep.* **1974**, *7679*.
8. Nash, G.E.; Glicksman, M.E. Capillary-limited steady-state dendritic growth: I. Theoretical development. *Acta Metall.* **1974**, *22*, 1283–1290. [CrossRef]
9. Langer, J.S.; Turski, L.A. Studies in the theory of interfacial stability: I. Stationary symmetric model. *Acta Metall.* **1977**, *25*, 1113–1119. [CrossRef]
10. Langer, J.S. Studies in the theory of interfacial stability: II. Moving symmetric model. *Acta Metall.* **1977**, *25*, 1121–1137. [CrossRef]

11. Alexandrov, D.V.; Galenko, P.K. Boundary integral approach for propagating interfaces in a binary non-isothermal mixture. *Phys. A* **2017**, *469*, 420–428. [CrossRef]
12. Galenko, P.K.; Alexandrov, D.V.; Titova, E.A. The boundary integral theory for slow and rapid curved solid–liquid interfaces propagating into binary systems. *Philos. Trans. R. Soc. A* **2018**, *376*, 20170218. [CrossRef]
13. Alexandrov, D.V.; Galenko, P.K. Selected mode for rapidly growing needle-like dendrite controlled by heat and mass transport. *Acta Mater.* **2017**, *137*, 64–70. [CrossRef]
14. Saville, D.A.; Beaghton, P.J. Growth of needle-shaped crystals in the presence of convection. *Phys. Rev. A* **1988**, *37*, 3423–3430. [CrossRef]
15. Titova, E.A.; Alexandrov, D.V. The boundary integral equation for curved solid–liquid interfaces propagating into a binary liquid with convection. *J. Phys. A Math. Theor.* **2022**, *55*, 055701. [CrossRef]
16. Alexandrov, D.V.; Bashkirtseva, I.A.; Ryashko, L.B. Nonlinear dynamics of mushy layers induced by external stochastic fluctuations. *Philos. Trans. R. Soc. A* **2018**, *376*, 20170216. [CrossRef]
17. Alexandrov, D.V.; Rakhmatullina, I.V.; Malygin, A.P. On the theory of solidification with a two phase concentration supercooling zone. *Russ. Metall. (Met.)* **2010**, *2010*, 745–750. [CrossRef]
18. Morse, P.M.; Feshbach, H. *Methods of Theoretical Physics*; Academic Press: Boston, MA, USA, 1953.
19. Korn, G.A.; Korn, T.M. *Mathematical Handbook for Scientists and Engineers: Definitions, Theorems, and Formulas for Reference and Review*; McGraw-Hill Book Company: New York, NY, USA, 1968.
20. Dash, S.K.; Gill, W.N. Foced convection heat and momentum transfer to dendritic structures (parabolic cylinders and paraboloids of revolution). *Int. J. Heat Mass Transf.* **1984**, *27*, 1345–1356.
21. Alexandrov, D.V.; Galenko, P.K. A review on the theory of stable dendritic growth. *Philos. Trans. R. Soc. A* **2021**, *379*, 20200325. [CrossRef]
22. Alexandrov, D.V.; Galenko, P.K. Selection criterion of stable mode of dendritic growth with n-fold symmetry at arbitrary Péclet numbers with a forced convection. In *IUTAM Symposium on Recent Advances in Moving Boundary Problems in Mechanics*; Springer: Cham, Switzerland, 2019; pp. 203–215.
23. Deguen, R.; Alboussière, T.; Brito, D. On the existence and structure of a mush at the inner core boundary of the Earth. *Phys. Earth Planet. Inter.* **2007**, *164*, 36–49. [CrossRef]
24. Alexandrov, D.V.; Britousova, A.V. Interdendritic spacing in growth processes with a mushy layer. *AIP Conf. Proc.* **2014**, *1648*, 850101.
25. Toropova, L.V.; Alexandrov, D.V.; Rettenmayr, M.; Liu, D. Microstructure and morphology of Si crystals grown in pure Si and Al-Si melts. *J. Phys. Condens. Matter* **2022**, *34*, 094002. [CrossRef] [PubMed]
26. Alexandrov, D.V.; Galenko, P.K. The shape of dendritic tips. *Philos. Trans. R. Soc. A* **2020**, *378*, 20190243. [CrossRef] [PubMed]
27. Galenko, P.K.; Danilov, D.A. Model for free dendritic alloy growth under interfacial and bulk phase nonequilibrium conditions. *J. Cryst. Growth* **1999**, *197*, 992–1002. [CrossRef]
28. Galenko, P.K.; Danilov, D.A. Selection of the dynamically stable regime of rapid solidification front motion in an isothermal binary alloy. *J. Cryst. Growth* **2000**, *216*, 512–526. [CrossRef]
29. Starodumov, I.O.; Titova, E.A.; Pavlyuk, E.V.; Alexandrov, D.V. The tip of dendritic crystal in an inclined viscous flow. *Crystals* **2022**, *12*, 1590. [CrossRef]
30. Brener, E.A.; Mel'nikov, V.A. Pattern selection in two-dimensional dendritic growth. *Adv. Phys.* **1991**, *40*, 53–97. [CrossRef]
31. Buyevich, Y.A.; Mansurov, V.V.; Natalukha, I.A. Instability and unsteady processes of the bulk continuous crystallization. *Chem. Eng. Sci.* **1991**, *46*, 2573–2588. [CrossRef]
32. Makoveeva, E.V.; Alexandrov, D.V. Mathematical simulation of the crystal nucleation and growth at the intermediate stage of a phase transition. *Russ. Metall. (Met.)* **2018**, *2018*, 707–715. [CrossRef]
33. Makoveeva, E.V.; Alexandrov, D.V. On the theory of phase transformation process in a binary supercooled melt. *Eur. Phys. J. Spec. Top.* **2020**, *229*, 375–382. [CrossRef]
34. Makoveeva, E.; Alexandrov, D.; Ivanov, A. Mathematical modeling of crystallization process from a supercooled binary melt. *Math. Methods Appl. Sci.* **2021**, *44*, 12244–12251. [CrossRef]
35. Barlow, D.A.; LaVoie-Ingram, E.; Bayat, J. Population-balance study of protein crystal growth from solution using a hyperbolic rate law. *J. Cryst. Growth* **2022**, *578*, 126417. [CrossRef]
36. Alexandrov, D.V.; Ivanov, A.A.; Nizovtseva, I.G.; Lippmann, S.; Alexandrova, I.V.; Makoveeva, E.V. Evolution of a polydisperse ensemble of spherical particles in a metastable medium with allowance for heat and mass exchange with the environment. *Crystals* **2022**, *12*, 949. [CrossRef]
37. Toropova, L.V.; Alexandrov, D.V. Dynamical law of the phase interface motion in the presence of crystals nucleation. *Sci. Rep.* **2022**, *12*, 10997. [CrossRef]
38. Alexandrov, D.V.; Toropova, L.V. The role of incoming flow on crystallization of undercooled liquids with a two-phase layer. *Sci. Rep.* **2022**, *12*, 17857. [CrossRef]
39. Peppin, S.S.L.; Aussillous, P.; Huppert, H.E.; Worster, M.G. Steady-state mushy layers: Experiments and theory. *J. Fluid Mech.* **2007**, *570*, 69–77. [CrossRef]
40. Alexandrov, D.V. Solidification with a quasiequilibrium two phase zone. *Acta Mater.* **2001**, *49*, 759–764. [CrossRef]

41. Alexandrov, D.V.; Aseev, D.L. One-dimensional solidification of an alloy with a mushy zone: Thermodiffusion and temperature-dependent diffusivity. *J. Fluid Mech.* **2005**, *527*, 57–66. [CrossRef]

42. Kerr, R.C.; Woods, A.W.; Worster, M.G.; Huppert, H.E. Solidification of an alloy cooled from above Part 1. Equilibrium growth. *J. Fluid Mech.* **1990**, *216*, 323–342. [CrossRef]

43. Alexandrov, D.V.; Aseev, D.L.; Nizovtseva, I.G.; Huang, H.-N.; Lee, D. Nonlinear dynamics of directional solidification with a mushy layer. Analytic solutions of the problem. *Int. J. Heat Mass Transf.* **2007**, *50*, 3616–3623. [CrossRef]

44. Nizovtseva, I.G.; Starodumov, I.O.; Pavlyuk, E.V.; Ivanov, A.A. Mathematical modeling of binary compounds with the presence of a phase transition layer. *Math. Methods Appl. Sci.* **2021**, *44*, 12260–12270. [CrossRef]

45. Saeed, T.; Abbas, I. Finite element analyses of nonlinear DPL bioheat model in spherical tissues using experimental data. *Mech. Based Des. Struct. Mach.* **2022**, *50*, 1287–1297. [CrossRef]

46. Alexandrov, D.V.; Zubarev, A.Y. Patterns in soft and biological matters. *Philos. Trans. R. Soc. A* **2020**, *378*, 20200002. [CrossRef] [PubMed]

47. Abbas, I.A.; Abdalla, A.E.N.N.; Alzahrani, F.S.; Spagnuolo, M. Wave propagation in a generalized thermoelastic plate using eigenvalue approach. *J. Therm. Stress.* **2016**, *39*, 1367–1377. [CrossRef]

48. Alexandrov, D.V.; Zubarev, A.Y. Heterogeneous materials: Metastable and non-ergodic internal structures. *Philos. Trans. R. Soc. A* **2019**, *377*, 20180353. [CrossRef]